Synthesis and characterization of Gallium-based materials for catalytic applications

Pedro Alexandre Lopes Martins
Instituto Superior Técnico, Universidade de Lisboa, Portugal

Abstract

In this work, gallium-cerium bimetallic oxides with three molar ratios (Ga:Ce=1:3, 1:1 and 3:1) were prepared by two methods: electrospinning technique and sol-gel method (epoxide addition method), aiming at the synthesis of compounds with different morphologies (fibres or aerogels) and to test them as catalysts for ODHE. Besides, to investigate the effect on this reaction, copper oxide supported on Ga_2O_3, CeO_2 and Ga:Ce (1:1) bimetallic oxide aerogels were also prepared. The catalytic performance for ODHE depends on the type of oxidant used, catalyst morphology, crystallite size and catalysts' acid-base properties. Among the bimetallic Ga-Ce oxides, the best results were those obtained over the fibres with the highest molar ratio, with 87% of ethane conversion and 13% of ethylene yield at 650 ºC. Moreover, the copper-based materials, especially the one supported on CeO2 presented the highest catalytic performance, with 97% ethane conversion and 7% ethylene yield at 650ºC. This confirms that copper has an enhanced effect on the catalyst's behaviour, as well as gallium. To our knowledge, this is the first time that such type of results using gallium-based catalysts are reported in the literature.

Keywords: Gallium, Cerium, Copper, Bimetallic oxides, ODHE, Ethylene.

1. Introduction

Gallium-based materials have been emerged as effective catalysts for some important catalytic reactions, such as selective reduction of NO_x removal using hydrocarbons,[1] dehydration of pentanediol,[2] hydrogenation of CO_2 to methanol,[3] reverse of water gas shift (RWGS),[4] methanol conversion into hydrocarbons,[5] and dehydrogenation of paraffins to olefins.[6]

Taking all this information into account, this work aims were: a) the development and characterization of gallium oxide-based materials and b) to test them as catalysts for the oxidative dehydrogenation of ethane (ODHE). The product desired for this reaction, ethylene (C_2H_4), is a key intermediate to produce other value chemicals such as ethylbenzene, acetaldehyde, acetic acid, styrene, ethanol, among others.[7] The demand of ethylene has been growing over the decades, reaching >200 million metric tons in 2020 and estimating to reach 300 million metric tons by 2025.[8] Additionally, the effect of different oxidants used for this reaction, like N_2O or CO_2, has been considered to replace O_2. This has several benefits, namely: a) the valorisation of anthropogenic pollutants as oxidants in ODHE can be a way to reduce green-house gases emissions and b) to create an environmental added value for such gaseous pollutants.

Nakagawa et al. have shown the good catalytic efficiency of gallium oxide-based in the presence of CO_2.[9] Nevertheless, Ga_2O_3 main drawback is his rapidly deactivation, but it becomes much more active and stable when together with other oxides.[10] Zhao et al.[11] have demonstrated that the addition

of CeO_2 increases the oxygen vacancies on Ga_2O_3, while Fe, Cu, Co, Mo, and V are said to promote redox reactions, which may have an impact on ODHE.[12]

Herein, gallium-cerium bimetallic oxides, with different ratios, were synthesized by two methods, the electrospinning technique and the epoxide addition method aiming the preparation of fibers and aerogels, respectively. Moreover, to study its influence on this reaction, copper oxide (CuO) was supported on Ga_2O_3, CeO_2 and Ga-Ce bimetallic oxide with a 1:1 molar ratio aerogel.

2. Experimental methods

2.1. Synthesis of gallium-based catalysts

In this work, gallium-cerium bimetallic oxides were prepared with three molar ratios of Ga_2O_3 and CeO_2, namely Ga_2O_3-6CeO_2, Ga_2O_3-2CeO_2, 3Ga_2O_3-2CeO_2 — which, from now on, will be referred as Ga:Ce (1:3), (1:1), and (3:1), respectively. Moreover, aiming to study the morphology influence on their performance, two synthesis methods were employed: the epoxide addition method, for the production of aerogels and the electrospinning technique, which leads to the formation of fibres.

2.1.1. Epoxide addition method

This method allows the preparation of aerogels using salts as precursors, namely: cerium chloride heptahydrate and gallium nitrate hydrate (Aldrich chemistry, 99%; ThermoFisher, 99.9% purity, respectively) that were completely dissolved in absolute ethanol (Fisher Chemical ≥ 99.8%), in the pretended ratios, at room temperature. Following which, propylene oxide (Acros Organics, 99,5% purity) was slowly added to the solution so that the ratio between moles of metals and propylene oxide was 1:9. The solution was stirred for another five minutes, after which it was allowed to stand until gel formation. Afterwards the gel was aged in absolute ethanol and sealed in its container for 48 hours at 50 °C, following which it was dried by the organic solvent sublimation drying (OSSD) using mixtures of acetonitrile and ethanol at 50, 80, and 100% (v/v), respectively at 50 °C.[13] Finally, the aerogel was calcined at 800 °C for 2 hours, using a heating rate of 1 °C/min and grounded to achieve a grain size of 200 mesh (75 µm).

2.1.2. Electrospinning technique

This method allows the preparation of fibres and for that solutions were prepared by dissolving 42wt.% of polyvinylpyrrolidone (PVP) in 50 mL absolute ethanol (Fisher Chemical ≥ 99.8%) followed by the addition of 4 mmol of cerium and gallium (III) nitrates (Aldrich, 99.9 % purity, hexahydrate; ThermoFisher, 99.9% purity, respectively) in the three pretended ratios. These solutions were then collected in a syringe with a ≈0.9 mm interior diameter stainless steel flat-tip needle and pumped continuously using a syringe pump (KW scientific) at a rate of 1 mL/h and applying an electric field of 16 kV applied between the syringe tip needle and a collector, in this case, a grounded aluminium foil placed at 10 cm from the needle tip. Finally, the collected electrospun material was calcined at 800 °C for 2 hours, under a heating rate of 1 °C/min.

2.1.3. Incipient wetness impregnation

In this work, Ga_2O_3, CeO_2 and Ga:Ce (1:1) aerogels were used as supports for the impregnation of copper oxide. For this, copper (II) nitrate hexahydrate (AlfaAesar, 98% purity) was dissolved in

distilled water, so that the equivalent mass of copper represented 25% of the total mass of the impregnated catalyst. Then, the solution was poured into a crucible containing the support and, under constant stirring, left to dry at 60 °C. After the water has completely evaporated, the catalyst was calcined at 500 °C for 2 hours under a heating rate of 1 °C/min and grounded to achieve a grain size of 200 mesh (75 µm).

2.2. Characterization methods

After the synthesis of the catalysts, a complete characterization of their physical and chemical properties is essential to a better understanding of the role of each element and structure of each catalyst in the reaction studied in this work.

The samples surface morphology was recorded using a benchtop SEM Phenom ProX G6 with CsB6 filament, operating at 15 keV and 74 µA and the surface chemical composition was determined by EDS using a B-U Bruker Quantax 400 EDS-SDD system. The crystalline structure was analysed using a D2Phaser Bruker diffractometer (Cu, kα monochromatic radiation, λ=1.5406 Å), with the operational settings for all scans being voltage=30kV voltage, current=10mA, and 2θ scan range between 20-80° using a step size of 0.03° with a time per step of 3.5 s. To study their reducibility, Temperature programmed reduction (TPR) studies were performed using the Micrometrics ChemiSorb 2720 – ChemiSoft TPx system, a specific Micromeritics quartz type U reactor, and a mixture of 10% H_2 in argon, total flow of 20 mL/min, at a heating rate of 10 ºC/min from room temperature to 1050 °C. Based on prior calibration measurements with NiO powders (Aldrich, 99.99995% purity), the integration of the experimental H_2–TPR curves allow to assess quantitative H_2-uptakes. Brunauer−Emmett−Teller (BET) method was used to measure the catalysts specific surface areas on the basis of nitrogen adsorption isotherm measurements at 77 K. Typically, data from the 0.05 to 0.3 relative pressure range are employed.[14] The measurements (monopoint) were conducted using a Micrometrics ChemiSorb 2720 – ChemiSoft TPx system. Under a flux of 30% N_2 in helium ($P/P_0 = 0.3$) of 20 mL/min, the catalysts were submitted to 3 cycles of N_2 adsorption (using liquid nitrogen, negative peaks) and desorption (when the liquid nitrogen is removed and the sample is allowed to return to room temperature, positive peaks). The specific surface areas measured by the BET method (SSA) are presented in Table 1.

Table 1: Specific surface areas measured by the BET method.

Catalyst		Specific Surface Area (m2/g)
Fibres		
Ga:Ce	1:3	15.9 ± 2.9
	1:1	23.8 ± 3.0
	3:1	29.1 ± 4.2
Aerogels		
CeO2		11.8 ± 0.7
Ga:Ce	1:3	3.5 ± 0.2
	1:1	6.8 ± 0.8
	3:1	7.4 ± 0.7
Ga2O3		25.5 ± 0.7
Impregnated		
25wt.%Cu/Ga:Ce		8.6 ± 0.1
25wt.%Cu/Ce		12.1 ± 0.7
25wt.%Cu/Ga		18.8 ± 0.9

Finally, in order to assess the acid-base properties of the catalysts, studies using a model reaction, the dehydrogenation/dehydration of 2-propanol (isopropanol) were undertaken. The tests were performed in a fixed-bed U-shaped Pyrex reactor at atmospheric pressure, in a temperature range between 175 to 275 °C. The reaction was conducted under a continuous flow of a mixture of 0.25% (v/v) of isopropanol in air N_2/O_2:80/20 (v/v) (Air Liquide, 99.9995% purity) with a Gas Hourly Space Velocity (GHSV) of 1012 mL/$g_{catalyst}$·h and a O_2 to isopropanol molar ratio of 10. Gas chromatography was used to analyse the composition of the reactor outlet gas. An Agilent 7280D chromatograph equipped with a flame ionization detector (FID) and a capillary column HP_PLOT_U, L = 25 m, ID = 0.32 mm was used for such purpose. From the ratio between the selectivity of acetone (νA) and propene (νP), a relative scale of basicity (νA/νP) was built.

2.3. Catalytic Measurements

ODHE studies were conducted with different oxidants (O_2, N_2O and CO_2), at atmospheric pressure, in the temperature range 400-700 ºC. The catalysts were placed in a U-shaped fixed bed quartz plug-flow reactor, which in turn was inserted into a tubular oven. The reaction temperature was controlled by a thermocouple placed near the catalytic bed. For the reaction itself, a gas mixture with C_2H_6, oxidant and He was used, molar ratio Oxidant/C_2H_6 of 10, together with a GHSV of 7500 mL C_2H_6/g of catalyst per hour (mL/g_{cat}·h) and, to prevent any diffusional problems, an optimized catalyst mass between 10-20 mg was used. To control each gas flows, mass flows controllers (Aalborg series A) were used. The reaction was followed by chromatography using a gas chromatograph, the Agilent 4890D GC, equipped with a TCD and a Restek ShinCarbon ST column (L = 2.0 m, Φ = 1/8 in, ID = 1mm, 100/200 mesh), the composition of the reactor outlet gas was analysed online. The catalytic activity, namely the C_2H_6 conversion, was evaluated employing the equations **1**-**4**. All reported results represent catalytic activity values after 1 hour of reaction.

$$C_2H_6\ conversion\ (\%) = \frac{[CO] + [CO_2] + [CH_4] + [C_2H_4]}{[CO] + [CO_2] + [CH_4] + [C_2H_4] + [C_2H_6]} \times 100 \quad (1)$$

$$CO_2\ selectivity\ (\%) = \frac{[CO_2]}{[CO] + [CO_2] + [CH_4] + [C_2H_4] + [C_2H_6]} \times 100 \quad (2)$$

$$C_2H_4\ selectivity\ (\%) = \frac{[C_2H_4]}{[CO] + [CO_2] + [CH_4] + [C_2H_4] + [C_2H_6]} \times 100 \quad (3)$$

$$C_2H_4\ yield\ (\%) = \frac{[C_2H_6]\ conversion \times [C_2H_4]\ selectivity}{[CO] + [CO_2] + [CH_4] + [C_2H_4] + [C_2H_6]} \times 100 \quad (4)$$

3. Results and Discussion

3.1. Catalyst's characterization

3.1.1. Morphology and composition: SEM/EDS

Figure 1a and **1b** shows SEM images of the Ga:Ce (1:1) fibres obtained by the electrospinning technique before and after the calcination treatment at 800 °C. SEM images of the aerogels prepared by the epoxide addition method show a spongy appearance that is very different from the fibres (**Figure 1c**). Regarding copper supported catalysts ($25_{wt.\%}$Cu), the SEM images show a needle-like structure can be seen that is typically associated with copper oxide, which was confirmed by EDS (**1d**).

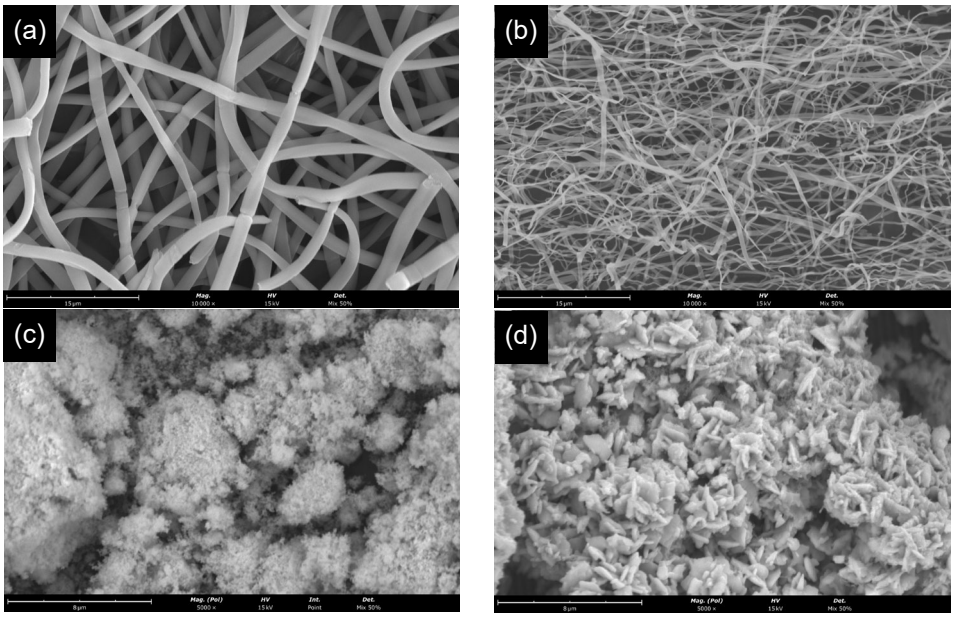

Figure 1: SEM images of Ga:Ce (1:1) fibres (a) before, and (b) after calcination at 800 °C (magnification 10 000x), (c) CeO_2 aerogel, and (d) $25_{wt.\%}$Cu impregnated on Ga:Ce (1:1) (magnification 5 000x).

3.1.2. Powder X-ray diffraction

Pure Ga_2O_3 and CeO_2 present diffraction patterns consistent with the ones present in the ICSD (Inorganic Crystal Structure Database) – ICSD 83645 and ICSD 88759 for the monoclinic phase of β–Ga_2O_3 and cubic phase of CeO_2, respectively. The diffraction pattern of the Ga-Ce bimetallic oxides (1:3) only show those peaks corresponding to CeO_2. β–Ga_2O_3 peaks are visible in Ga:Ce (3:1) and (1:1), but they are weak, which could be due amorphization or X-ray inaccessibility due to incorporation of Ga^{3+} cations into cerium oxide cubic structure either by simple insertion in its interstices or by Ce^{4+} substitution. Regarding the $25_{wt.\%}$Cu supported materials, they show the diffraction patterns of the supports and additionally the diffraction patterns of CuO (monoclinic phase, ICSD 43179), as shown in **Figure 2c**.

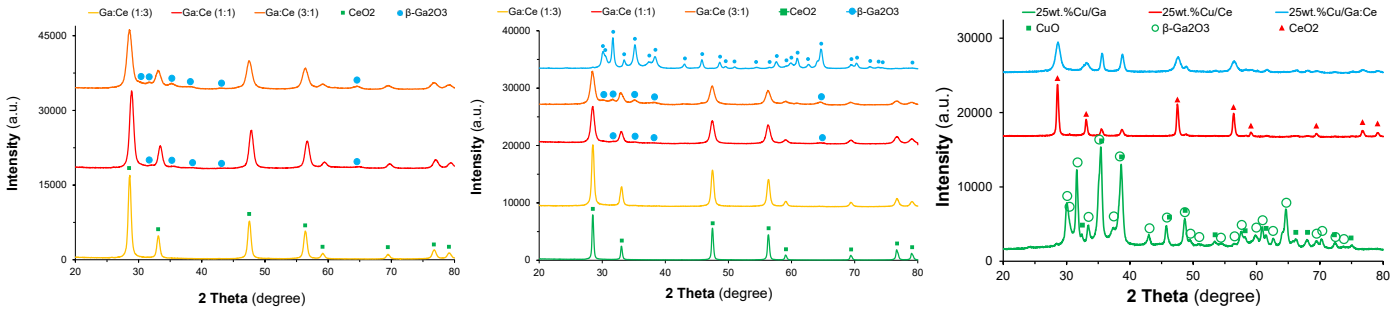

Figure 2: XRD patterns of Ga:Ce bimetallic oxides (a) fibres, (b) aerogels and pure CeO_2 and Ga_2O_3 aerogels, and (c) 25wt.%Cu supported materials after calcination.

Moreover, the lattice parameters of the bimetallic oxides calculated from the XRD patterns (**Figure 3**) seem to confirm the formation of a CeO_2–Ga_2O_3 solid solution, which can be a substitutional or interstitial type.[15] In fact, the ionic radius of Ga^{3+} being inferior to that of Ce^{4+} or Ce^{3+} (0.62 versus 0.97 or 1.01 Å, respectively)[16] explains the lattice deviation from the pure CeO_2 materials synthesized by each method. It is known from the literature that a complete substitution is only possible if the host ion

and the substitutional ion have a similar size.[15] Therefore, due to the large difference in ionic radius between Ce^{4+} and Ga^{3+}, there seems to be a limit for the Ce^{4+} substitution by Ga^{3+}, which in the literature is reported to be near 25 % mol/mol of Ga.[2,17] The results from this work suggest that this limit may be higher, closer to 33% in the case of the aerogels and closer to 50% in the case of the fibres.

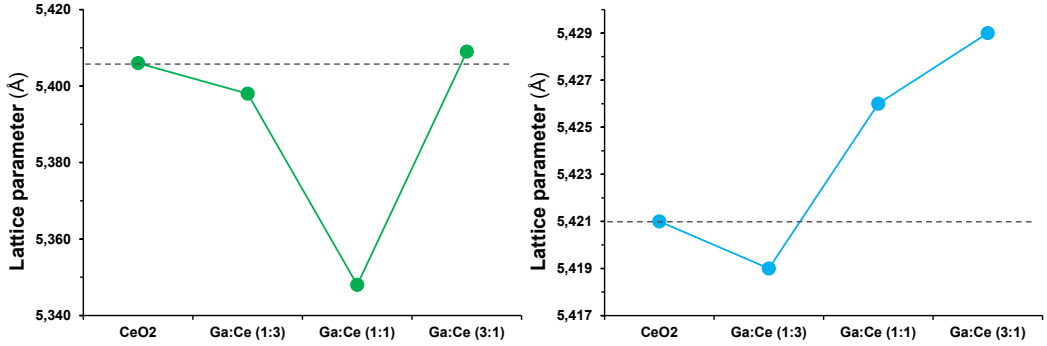

Figure 3: Ga-Ce bimetallic oxides lattice parameter evolution for (a) fibres and (b) aerogels: comparison with pure CeO_2.

3.1.3. Oxide phases reducibility and stability

H_2–TPR profile of Ga_2O_3 aerogel (**Figure 4b**) present a small peak at 469 °C which others authors have associated to its surface reduction into GaH_x species[18] and formation of oxygen vacancies sites.[19] This, however, is not significant since its XRD patterns obtained after H_2–TPR does not show an oxide phase change. These GaH_x species reoxidize upon cooling to room temperature,[18] which corroborates reports saying that β–Ga_2O_3 is hardly reducible[20] and its H_2–TPR profile does not present any significant H_2 consumption peak.[19,21] Regarding pure CeO_2, the first peak at 430 °C is also reported to be related to easily reducible surface oxygen of cerium oxide, while the second peak at 784 °C is associated with bulk reduction of CeO_2 to Ce_2O_3.[2,22] Just like in the case of β–Ga_2O_3, the XRD pattern after H_2–TPR does not show any phase change in the material, thus the reduction being complete at the bulk seems non-existent at a surface easily oxidized as soon as the materials enter in contact with air. Concerning the Ga-Ce bimetallic oxides, fibres, and aerogels similar compositions generated slightly different profiles, as shown in **Figure 4a** and **4b**, probably due to their different morphologies and surface areas.[23] It is noticeable that the addition of more gallium into cerium oxide shifts the peak associated with bulk reduction of CeO_2 to lower temperatures, more visible for the samples with higher CeO_2 content, 734 versus 784 °C or 761 versus 784 °C, for the fibres or aerogels, respectively. Accordingly with the literature that could be assigned to a contribution of gallium to improve the reducibility of CeO_2.[2,22] About the copper supported catalysts (**Figure 4c**), new peaks appears at 184 and 241 °C that can be assigned to the reduction of CuO to metallic copper,[24] while the peak at 208 °C is related to the formation of a Cu-Ga intermetallic phase (Ga_4Cu_9) in $25_{wt.\%}Cu/Ga_2O_3$.

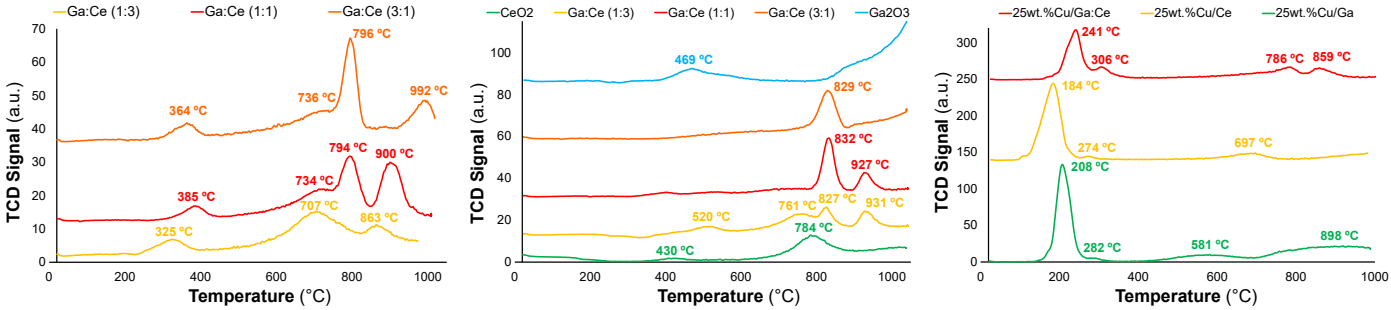

(a) (b) (c)

Figure 4: H_2–TPR profiles of CeO_2 and Ga_2O_3 particles and of the 3 Ga:Ce ratios (a) fibres, (b) aerogels and (c) copper supported materials.

3.2. Catalytic Studies

To access the influence of the oxidant in ODHE, Ga:Ce (1:1) aerogel was tested in three oxidants: molecular oxygen (O_2), nitrous oxide (N_2O) and carbon dioxide (CO_2); across a range of temperatures (**Figure 5a**). The best results are those obtained with N_2O as oxidizing agent: higher conversion of ethane and higher yields for ethylene across all range of temperatures studied. Therefore, it was decided to conduct further tests under N_2O. Then, the study of the N_2O/C_2H_6 molar ratio was performed over $25_{wt.\%}Cu/Ga_2O_3$. This is an important parameter in order to optimize reaction performance. It is possible to see that by increasing this value, the C_2H_6 conversion rises until it reaches a maximum conversion at N_2O/C_2H_6=10 (**Figure 5b**). Hence, further studies were done under this condition.

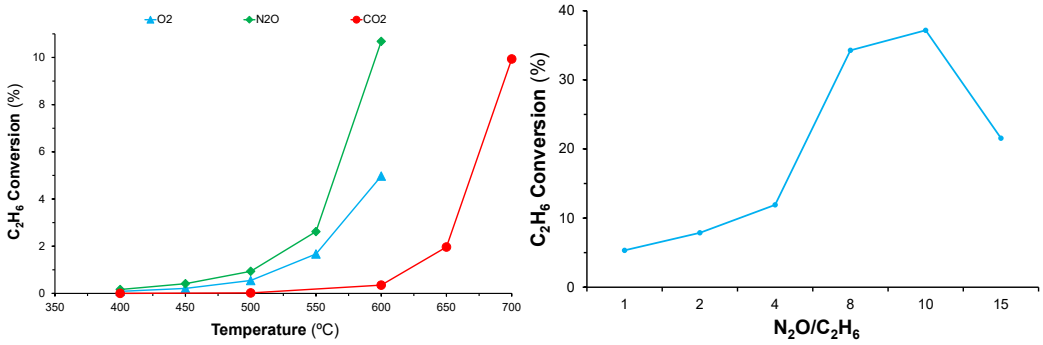

(a) (b)

Figure 5: Oxidant effect: (a) ethane conversion, using Ga:Ce (1:1) aerogel as catalyst (Oxidant/C_2H_6=10, GHSV=7500 mL $C_2H_6/g_{cat}.h$), and (b) N_2O/C_2H_6 molar ratio effect evolution, using $25_{wt.\%}Cu/Ga_2O_3$ (GHSV=7500 mL $C_2H_6/g_{cat}.h$, T=550 °C).

As expected, the increase of temperature is followed by the raise of C_2H_4 selectivity (**Figure 6**). It is clear that the best results are those obtained over the fibres, which present higher ethane conversion and higher ethylene selectivity and yield. The best results among the aerogels are those obtained over pure metal oxides, cerium and gallium, that unfortunately were not possible to prepare as fibres. Comparing to the Ga-Ce bimetallic oxides, the addition of gallium to cerium oxide has a positive effect, contributing to increase the ethylene selectivity. Moreover, blank tests were performed without catalysts (not shown for clarity purposes) show that C_2H_6 conversions and C_2H_4 yields are residual until 550 °C (≤ 0.7%), becoming significative at temperatures > 600 °C (≥ 6%). Thus, for comparison purposes in the kinetic regime we have use only the results obtained at 550 °C.

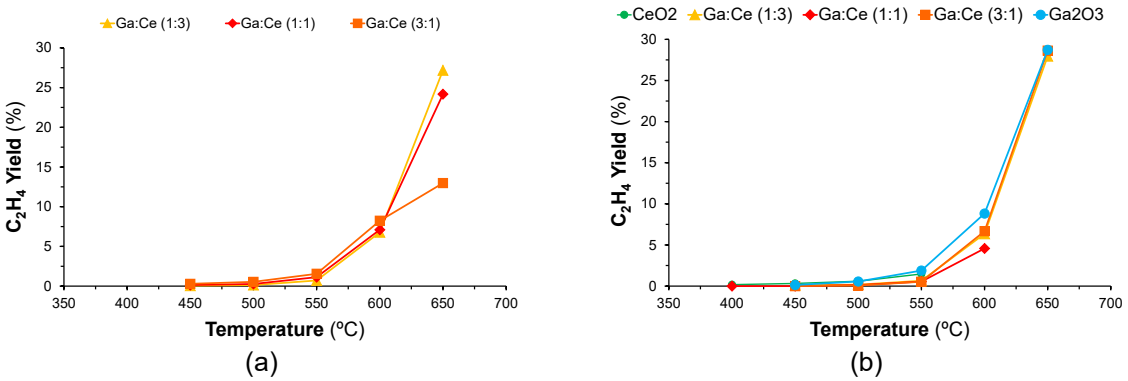

Figure 6: Effect of temperature on ODHE reaction over (a) fibres and (b) aerogels regarding C_2H_6 yield (N_2O/C_2H_6=10, GHSV=7500 mL $C_2H_6/g_{cat}.h$).

As for the copper-based materials, these exhibited the best results among all materials prepared in this work. In particular, the copper supported catalyst on gallium presents the highest activity towards ethylene (**Figure 7**).

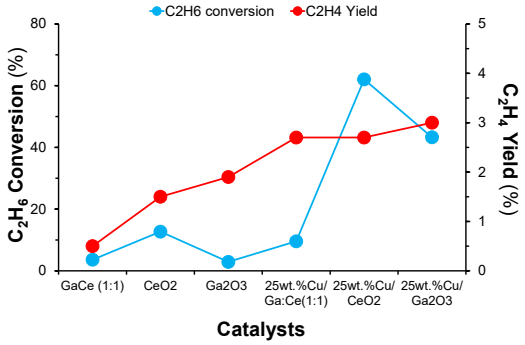

Figure 7: $25_{wt.\%}Cu$ supported materials and their respective supports, in respect of their C_2H_6 conversion and C_2H_4 and CO_2 selectivity (N_2O/C_2H_6=10, GHSV=7500 mL $C_2H_6/g_{cat}.h$, T=550 °C).

The evolution of the ethylene yield, measured at 550 °C, with the catalysts' crystallite sizes is presented in **Figure 8**. It was found that the smaller the crystallite size (CeO_2 for the bimetallic oxides and CuO for the copper-based materials), the better is the catalytic activity for the production of ethylene. Moreover, as the Ga content rises, the C_2H_4 yield increases, which confirm the conclusions reported before for the temperature effect.

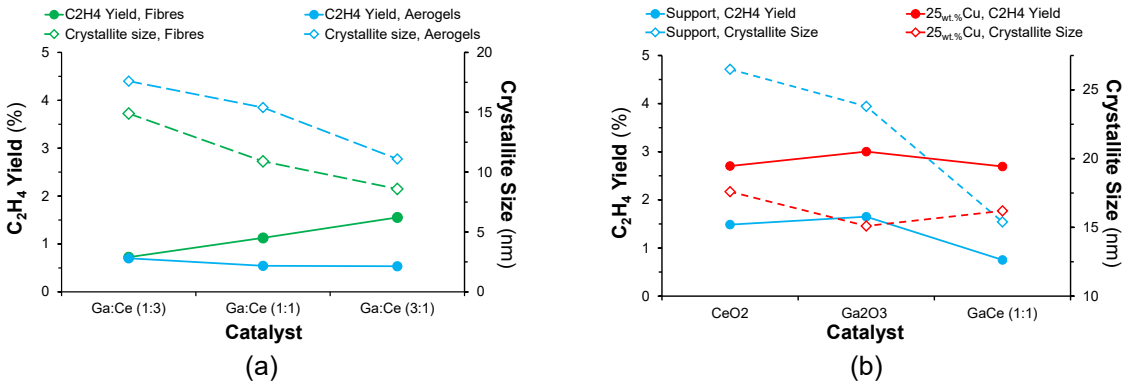

Figure 8: Effect of the active phase's crystallite size of (a) Ga-Ce bimetallic oxides and (b) 25wt.%Cu supported materials regarding C_2H_4 yield.

Gärtner et al.[25] related a higher concentration of basic sites to a higher ethane dehydrogenation, whereas acid sites favour ethane oxidation. The results obtained in this work are in line with these statements. It is possible to observe a trend common to both the aerogels and fibres showing the higher

the basicity, the higher the yield towards C_2H_4 (**Figure 9a**). It is also important to stress that although the basicity of CeO_2 is higher and ethylene yield lower than those measured over Ga_2O_3 (14 and 1.5% versus 7 and 1.9%, respectively), the higher the gallium content, the higher the basicity and activity, which seems to confirm the existence of a synergetic interaction between gallium and cerium already pointed by the XRD analysis that appear to indicate the formation of a CeO_2–Ga_2O_3 solid solution, mainly of the substitutional type. Regarding the copper supported materials and the basicity effect on the yield to ethylene, it is difficult to find a specific trend since the decrease in basicity is not followed by an unquestionable decrease of the yields for ethylene (**Figure 9b**).

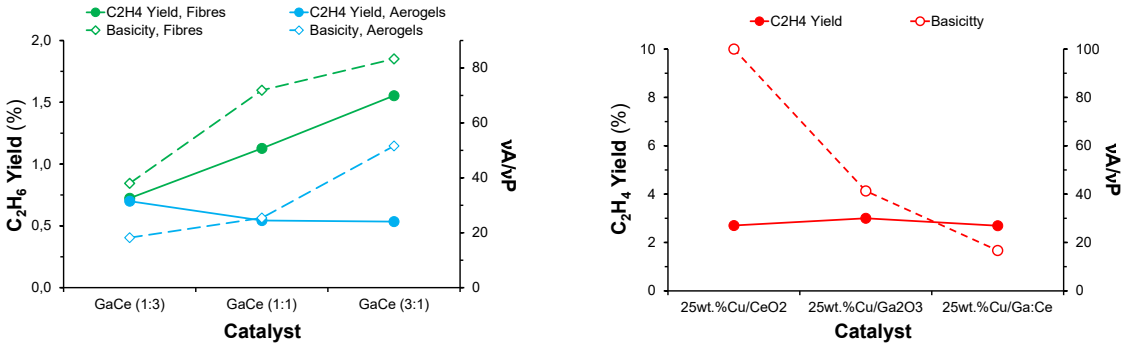

Figure 9: Effect of acid-base properties (a) Ga-Ce bimetallic oxides and (b) 25wt.%Cu supported materials regarding C_2H_4 yield. (N_2O/C_2H_6=10, GHSV=7500 mL C_2H_6/gcat.h, T=550 °C).

4. Conclusions

The two different morphologies were successfully obtained: the aerogels prepared by the epoxide addition method that present a spongy appearance, which is very different from the fibres obtained by electrospinning technique. These materials are better described as oxide solid solutions of gallium-cerium that arise from Ga^{3+} incorporation on the CeO_2 matrix, by substitution of Ce^{4+}, which increases the synergetic interaction between the two metals and contribute to its better catalytic behaviour compared to pure metal gallium and cerium oxides. Moreover, H_2-TPR studies allowed to understand how the pure oxide (Ga_2O_3 and CeO_2) were unable to reduce, while the bimetallic oxides proved that gallium insertion into CeO_2 matrix facilitated its reduction and, inclusive, the formation of a perovskite phase ($CeGaO_3$). Some reports had already studied the formation of this perovskite, however in this work, an easier path to obtain this material with a good purity is presented.

The catalytic studies for dehydrogenation of ethane, aiming to the production of a value-added chemical such as ethylene, showed a good catalytic behaviour for the Ga-Ce bimetallic oxides that depends on the type of oxidant, catalyst morphology, crystallite size and catalysts acid-base properties, namely their basicity. The best results were those obtained with N_2O using fibres, namely those with the highest gallium content (Ga-Ce molar ratio 3:1), with 87% of ethane conversion and 13% of ethylene yield at 650 ºC. Furthermore, with the introduction of copper, the catalysts activity increases significantly, especially over copper supported on CeO2, with 97% ethane conversion and 7% ethylene yield at 650ºC, showing that copper has an enhanced effect on the catalyst's behaviour. It was also found that the catalytic activity depends on the crystallites size and catalysts acid-base properties and as expected, the smaller the crystallite sizes and the higher the basicity, the higher the catalytic activity towards ethylene. To our knowledge, this is the first time that such type of results using gallium-based catalysts are reported in the literature.

References

[1] T. Watanabe, Y. Miki, Y. Miyahara, T. Masuda, H. Deguchi, H. Kanai, S. Hosokawa, K. Wada, M. Inoue, *Catal. Lett.* **2011**, *141*, 1338.
[2] M. K. Gnanamani, G. Jacobs, W. D. Shafer, S. D. Hopps, B. H. Davis, *ChemistrySelect* **2017**, *2*, 4150.
[3] S. E. Collins, M. A. Baltanás, J. J. Delgado, A. Borgna, A. L. Bonivardi, *Catal. Today* **2021**, *381*, 154.
[4] H. Dai, A. Zhang, S. Xiong, X. Xiao, C. Zhou, Y. Pan, *ChemCatChem* **2022**, *14*, DOI 10.1002/cctc.202200049.
[5] D. Freeman, R. P. K. Wells, G. J. Hutchings, *J. Catal.* **2002**, *205*, 358.
[6] P. Castro-Fernández, D. Mance, C. Liu, I. B. Moroz, P. M. Abdala, E. A. Pidko, C. Copéret, A. Fedorov, C. R. Müller, *ACS Catal.* **2021**, *11*, 907.
[7] K. Nakagawa, C. Kajita, K. Okumura, N. Ikenaga, M. Nishitani-Gamo, T. Ando, T. Kobayashi, T. Suzuki, *J. Catal.* **2001**, *203*, 87.
[8] "Ethylene production capacity globally 2025," can be found under https://www.statista.com/statistics/1067372/global-ethylene-production-capacity/, **2022**.
[9] K. Nakagawa, M. Okamura, N. Ikenaga, T. Suzuki, K. Nakagawa, M. Okamura, T. Suzuki, T. Kobayashi, T. Kobayashi, *Chem. Commun.* **1998**, 1025.
[10] S. P. Batchu, H.-L. Wang, W. Chen, W. Zheng, S. Caratzoulas, R. F. Lobo, D. G. Vlachos, *ACS Catal.* **2021**, *11*, 1380.
[11] B. Zhao, Y. Pan, C. Liu, *Catal. Today* **2012**, *194*, 60.
[12] S. Najari, *Chem Soc Rev* **2021**, 42.
[13] T. F. Baumann, A. E. Gash, J. H. Satcher, in *Aerogels Handb.* (Eds: M.A. Aegerter, N. Leventis, M.M. Koebel), Springer New York, New York, NY, **2011**, pp. 155–170.
[14] M. Jaroniec, M. Kruk, A. Sayari, in *Stud. Surf. Sci. Catal.* (Eds: L. Bonneviot, F. Béland, C. Danumah, S. Giasson, S. Kaliaguine), Elsevier, **1998**, pp. 325–332.
[15] W. D. Callister, *Materials Science and Engineering: An Introduction*, John Wiley & Sons, New York, **2007**.
[16] "Database of Ionic Radii," can be found under http://abulafia.mt.ic.ac.uk/shannon/ptable.php, **n.d.**
[17] S. Collins, G. Finos, R. Alcántara, E. del Rio, S. Bernal, A. Bonivardi, *Appl. Catal. Gen.* **2010**, *388*, 202.
[18] G. D. Meitzner, E. Iglesia, J. E. Baumgartner, E. S. Huang, *J. Catal.* **1993**, *140*, 209.
[19] P. Castro-Fernández, D. Mance, C. Liu, P. M. Abdala, E. Willinger, A. A. Rossinelli, A. I. Serykh, E. A. Pidko, C. Copéret, A. Fedorov, C. R. Müller, *J. Catal.* **2022**, *408*, 155.
[20] Z. Helali, A. Jedidi, O. A. Syzgantseva, M. Calatayud, C. Minot, *Theor. Chem. Acc.* **2017**, *136*, 100.
[21] L. Li, W. Wei, M. Behrens, *Solid State Sci.* **2012**, *14*, 971.
[22] E. L. Fornero, J. Vecchietti, M. Boucinha Rodrigues, J. C. Hernández-Garrido, A. L. Bonivardi, *Int. J. Hydrog. Energy* **2022**, *47*, 18018.
[23] F. Giordano, A. Trovarelli, C. de Leitenburg, M. Giona, *J. Catal.* **2000**, *193*, 273.
[24] R. Ladera, F. J. Pérez-Alonso, J. M. González-Carballo, M. Ojeda, S. Rojas, J. L. G. Fierro, *Appl. Catal. B Environ.* **2013**, *142–143*, 241.
[25] C. A. Gärtner, A. C. van Veen, J. A. Lercher, *ChemCatChem* **2013**, *5*, 3196.